Valley-Confinement and River-Tidal Controls on Channel Morphology Along the Fluvial to Marine Transition Zone of the Đồng Nai River System, Vietnam

Marcello Gugliotta[1]*, Yoshiki Saito[1,2], Thi Kim Oanh Ta[3] and Van Lap Nguyen[3]

[1] Estuary Research Center, Shimane University, Matsue, Japan, [2] Geological Survey of Japan, AIST, Tsukuba, Japan,
[3] HCMC Institute of Resources Geography, VAST, Ho Chi Minh City, Vietnam

Along the fluvial to marine transition zone (FMTZ) of river deltas, the river-tidal dynamics exert a primary control on channel width, sinuosity, and bed elevation; however, other local factors, such as valley confinements, bifurcations, and confluences, can modify the channel morphology. Here, we report a case study of the major channel of the Đồng Nai River System (DNRS) that shows complex morphological trends linked to multiple factors. This study is based on the analysis of satellite images and bathymetric maps of the studied channel, together with a digital elevation model of the area and additional climate and hydrology data. Our study shows that channel width, sinuosity, and bed elevation show mutual relationships and complex upstream to downstream trends linked to the river-tidal dynamics and valley confinements, together with more local effects due to bifurcations and confluences. The tidal dynamics is mainly responsible for the seaward-widening and seaward-shallowing trends and the abrupt decrease in channel sinuosity observed in the downstream tract of the channel, whereas the relatively constant channel width and sinuosity in the upstream tract suggest a control of the river dynamics. The studied channel also shows three areas of valley widening or exit, which are characterized by high channel sinuosity, the presence of minor and major bifurcations, and additional changes in channel width and bed elevation, and they are considered important nodes in this system. Valley-related nodes also show different active and inactive features, implying that the degree of activity and importance of these nodes likely varied through time, migrating from upstream to downstream due to the deltaic progradation.

Keywords: mesotidal, bedrock control, river valley, river mouth, river-tidal control

INTRODUCTION

River deltas represent some of the most important areas on Earth for their scientific, social, and economic significance, and they are threatened by numerous factors, including natural events, human activities, and climate change. Along their fluvial to marine transition zone (FMTZ), river deltas are characterized by a complex interaction of riverine and marine processes that

control morphology, sedimentation, and multiple other geological and non-geological aspects (e.g., Dalrymple and Choi, 2007; La Croix et al., 2015; Gugliotta et al., 2017). Here, the river-tidal dynamics exert a primary control on the channel morphology, producing distinct upstream-to-downstream trends in channel width, sinuosity, and bed elevation (Sassi et al., 2012; Guo et al., 2014; Gugliotta et al., 2017; Kästner et al., 2017; Yang et al., 2017; Nienhuis et al., 2018; Gugliotta and Saito, 2019), however, other local factors that are rarely taken into account, such as valley confinements, bifurcations, and confluences, can also modify the channel morphology, making trends along the FMTZ more complex and difficult to decipher. Constraining these trends and understanding the different controls on the channel morphology is crucial in order to address the present and future threats faced by these areas. Here, we report a case study of the major channel of the Đồng Nai River System (DNRS) that shows complex morphological trends linked to multiple factors. The objective of this paper is to understand the role of different controls on channel morphology along the FMTZ, highlighting the importance of local factors.

REGIONAL BACKGROUND

The DNRS is a relatively small river delta located near Ho Chi Minh City and to the north of the Mekong River delta, in the southern part of Vietnam (**Figure 1A**). Its drainage basin is approximately 46,000 km^2 (~1/18 of the Mekong drainage basin) and consists of a mountainous area on the northern and northeastern part and a coastal plain on the western and southwestern part (**Figure 1B**). The DNRS consists of the Đồng Nai River and a series of tributaries (e.g., Vàm Cỏ River, Saigon River) and distributaries (e.g., Soài Rạp River, Lòng Tàu River), which form a complex river-mouth system interfacing with the South China Sea (also called East Sea) (**Figure 1C**). The eastern part of the DNRS consists of the Can Gio Mangrove Biosphere Reserve (UNESCO site since 2000), a wetland with a dense mangrove forest and numerous tidal channels. The Trị An dam, which was built in 1986 for multipurpose and forms a reservoir of 2.7 km^3 (Dao et al., 2010), is present at approximately 145 km from the river mouth in the Đồng Nai River, whereas other dams are also present in the upstream parts of the tributary channels. A large part of the DNRS is confined within a valley bounded by uplands consisting of pre-Holocene sedimentary and igneous rocks (Kitazawa et al., 2006; Hennig et al., 2018). According to Fujimoto et al. (2011), the shoreline DNRS has prograded approximately 70–80 km in the last 7 kyr, partially exiting the upland-bounded valley.

CLIMATE AND HYDROLOGY

The study area is characterized by a tropical climate with relatively constant temperature through the year and a monsoon-driven seasonality mainly consisting of variations in amount of precipitation and in wind speed and direction. From 2012 to 2017, the monthly mean air temperature and monthly mean

humidity at Vũng Tàu ranged from 25°C to 30.6°C with an average of 28°C and from 71 to 85% with an average of 78%, respectively. In the same period, yearly rainfall at Vũng Tàu ranged from 1215.6 to 1709.7 mm, with the highest values from June to October, intermediate values in April, May, and November, and the lowest values from December to March (**Figure 2A**). The water discharge from the DNRS is strongly dependent on the seasonal rainfall, although can be affected by the dams (Nguyen et al., 2019). From 2012 to 2016, the average water discharge at Biên Hòa was 613 m^3/s with higher values from July to October and peak discharge in October (**Figure 2B**). River-related seasonal water-level fluctuations up to 1 m are observed at Biên Hòa, whereas these are little or absent at Nhà Bè and Vũng Tàu (**Figure 3**). Tide-related water-level fluctuations are perceptible up to the Trị An dam and are present throughout the year exceeding the 3 m during spring tide at the three stations (**Figure 3**). Marine-related seasonal water-level fluctuations exceed 1 m at Vũng Tàu, but they are minor at Nhà Bè and little or absent at Biên Hòa (**Figure 3**).

MATERIALS AND METHODS

This study focuses on the final 144 km of the Đồng Nai – Soài Rạp River of the DNRS, from the Trị An dam to the river mouth. Rainfall, humidity, and temperature data (from 2012 to 2017) at Vũng Tàu station were obtained from the General Statistics Office of Vietnam. Water discharge data (from 2012 to 2016) at Biên Hòa were obtained from Nguyen et al. (2019). Water-level data (2017) at Biên Hòa, Nhà Bè, and Vũng Tàu stations were obtained from the Southern Regional Hydrometeorological Center of Vietnam. The studied channel and its drainage basin were investigated using the software Quantum GIS and a digital elevation model (DEM) from the Shuttle Radar Topography Mission (SRTM) (from the United States Geological Survey), satellite images (from Google Earth Pro, Landsat/Copernicus, 2016), and bathymetric maps (from the United States Army, Corps of Engineers, 1965). All the measurements were carried out manually using the measuring tool of the software. River distance was measured along the mid-point axis of the channel starting from a chosen point at the river mouth. The DEM was used to map the distribution of uplands using the 5 m contour line as a reference and to measure the valley width for the upland-constrained part of the channel. Satellite images were used to measure channel width and sinuosity for the entire studied part of the channel. Bathymetric maps were used to measure channel bed elevation (mid-channel and maximum-depth points) for its final 102 km. Valley width, channel width, and channel bed elevation were measured with a spacing of 1 km. Channel sinuosity was calculated in terms of sinuosity index (SI) between inflection points for each single and composite channel bend. Averaged values of valley width, channel width, channel sinuosity, and channel bed elevation were calculated for each 5 km interval (i.e., 0–4 km, 5–9 km, etc.). Raw data can be found in the **Supplementary Table S1**. Note: although 2016 bathymetric maps are available, we decided to use 1965 bathymetric maps as
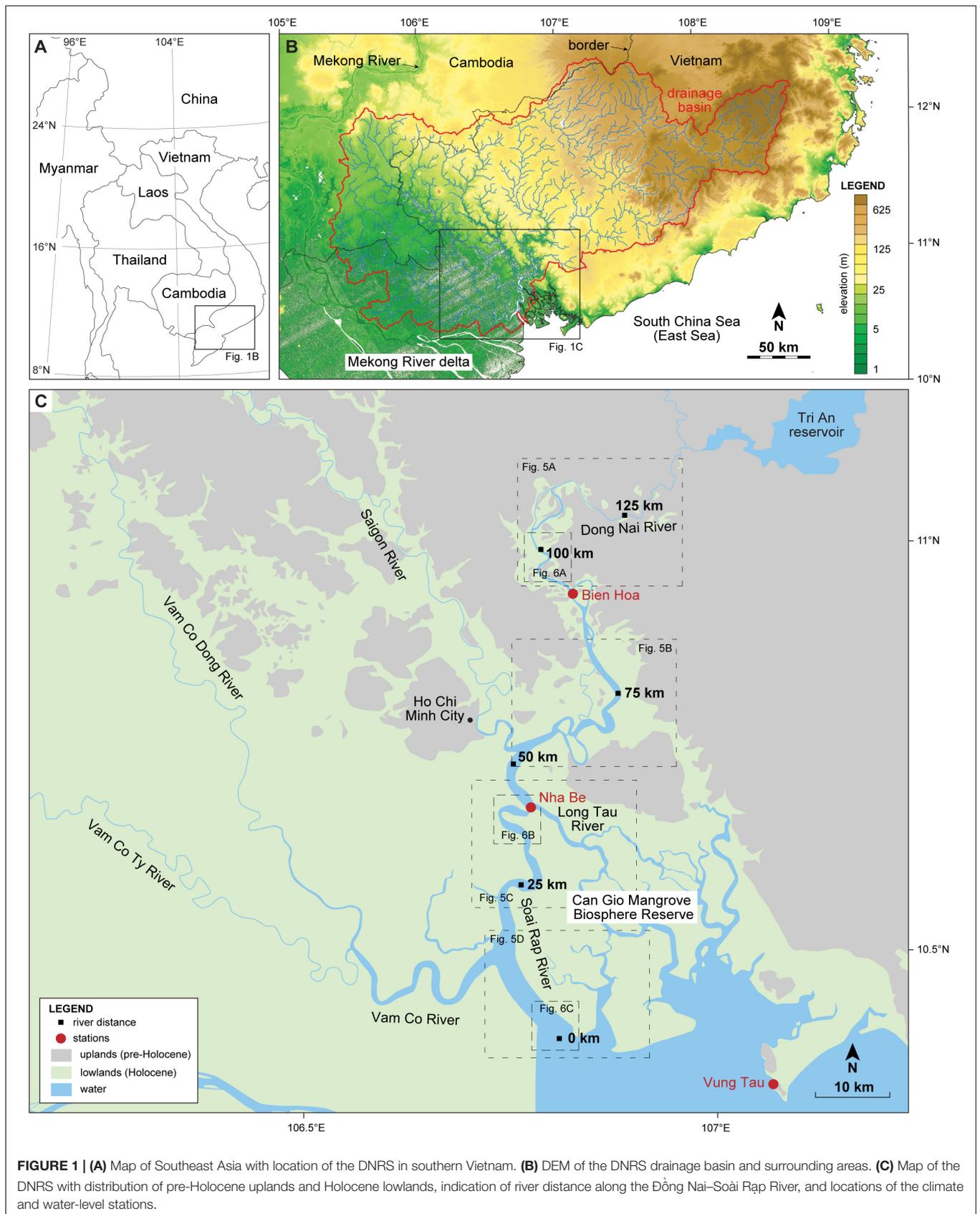
FIGURE 1 | (A) Map of Southeast Asia with location of the DNRS in southern Vietnam. (B) DEM of the DNRS drainage basin and surrounding areas. (C) Map of the DNRS with distribution of pre-Holocene uplands and Holocene lowlands, indication of river distance along the Đồng Nai–Soài Rạp River, and locations of the climate and water-level stations.

FIGURE 2 | (A) Minimum, average, and maximum monthly rainfall at Vũng Tàu from 2012 to 2017 (from the General Statistics Office of Vietnam). **(B)** Minimum, average, and maximum monthly mean water discharge at Biên Hòa from 2012 to 2016 (from Nguyen et al., 2019).
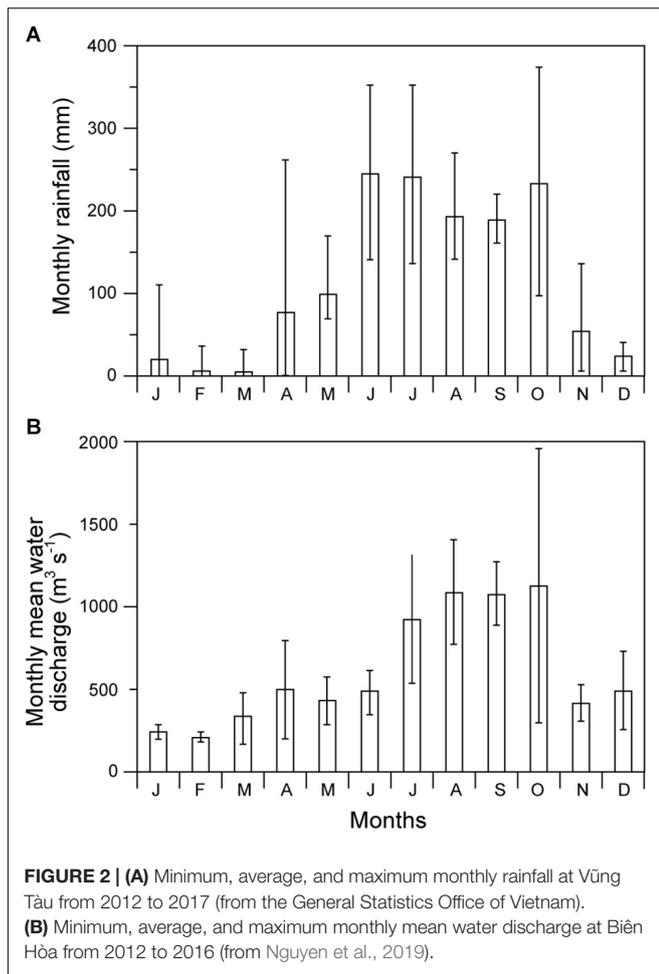
these cover a longer portion of the channel; within this time range the general trends described in this paper did not show significant variations.

RESULTS

Valley Width

Along the studied channel, valley width shows a step-like seaward increase (**Figures 4A,B**). Between 144 and 118 km from the river mouth, the valley is narrow, with an average of 0.29 km, making the channel entirely confined. At 117 km, valley width abruptly increases (**Figure 5A**), showing an average of 3.56 km between 117 km and 82 km, but the channel remains highly confined. Valley width increases again at 81 km and successively at 75 km (**Figure 5B**). The average valley width is 8.68 km between 81 km and 75 km and 13.43 km between 75 km and 51 km, making the channel highly and moderately confined, respectively. Near the Saigon River confluence, a local upland makes the valley anomalously narrower for a few kilometers. At 50 km, uplands become absent (**Figure 5C**), thus the channel is unconfined between 50 and 0 km (**Figure 5D**).

Channel Width

The studied channel shows constant width upstream and an exponentially-increasing seaward-widening trend downstream (**Figures 4C,D**). Between 144 and 120 km from the river mouth, channel width is relatively constant with an average of 0.21 km. At 119 km, in correspondence of the first area of valley widening, channel width shows a slight increase (**Figure 5A**). Between 119 and 96 km, channel width shows an increased average of 0.30 km, but no clear seaward widening (i.e., 0 m/km). At 96 km, channel width starts to increase seaward reaching the highest value of 5.54 km at the river mouth (**Figure 5D**). The average widening rate increases seaward being 7 m/km between 96 and 60 km, 17 m/km between 60 and 24 km, 102 m/km between 24 and 4 km, and 610 m/km between 4 and 0 km. Moreover, additional increases in channel width are also observed near the other areas of valley widening or exit (**Figures 4C,D, 5B,C**). Local increases and decreases in channel width are observed at the confluences of the Saigon River and Vàm Có River and at the bifurcation of the Lòng Tàu River, respectively.

Channel Sinuosity

The studied channel shows a complex trend with generally less variable and relatively constant sinuosity upstream and highly variable sinuosity downstream (**Figures 4E,F**). Between 144 and 95 km, channel sinuosity of single bends reaches SI values up to 1.67 and shows an average of 1.20. Between 95 and 0 km, channel sinuosity of single bends shows higher variability with SI reaching values up to 2.47 and showing an average of 1.38. Nonetheless, the majority of the high-sinuosity bends in both parts of the channel are located near the areas of valley widening or exit (**Figures 4E,F, 5A–C**). If these high-sinuosity bends are not taken into account, channel sinuosity is slightly lower in the downstream part of the channel compared to the upstream part. An abrupt decrease in SI value is observed at 95 km near the area of onset of channel widening. Single bends are sometimes arranged in composited bends with variable SI values that are also reported in **Figures 4E,F**.

Channel Bed Elevation

The studied channel shows relatively constant bed elevation upstream, highly variable bed elevation in the intermediate part, and a seaward-shallowing trend downstream (**Figures 4G,H**). No data are available between 144 and 103 km. Between 102 and 74 km, channel-bed elevation ranges from −4.7 to −12.2 m for both the mid-channel and maximum-depth points and shows averages of −7 m for the former and −8 m for the latter (**Figure 6A**). Between 75 and 35 km, channel-bed elevation shows a higher variability, with mid-channel values ranging from −6.6 to −25.9 m with average of −13 m and maximum-depth values ranging from −9.7 to −27.9 m with average of −15.9 m (**Figure 6B**). Between 35 and 0 km, the channel becomes shallower seaward, reaching at the river mouth mid-channel and maximum-depth values of −9.7 and −11.7 m, respectively (**Figure 6C**). In the intermediate part, the majority of the deeper areas are associated with the high-sinuosity bends and located near the areas of valley widening or exit

FIGURE 3 | (A–C) Water-level fluctuations at three stations in the study area (from the Southern Regional Hydrometeorological Center of Vietnam).
(D) Reconstructed spring high and low tide water-level profiles in February, June, and October for the studied channel.
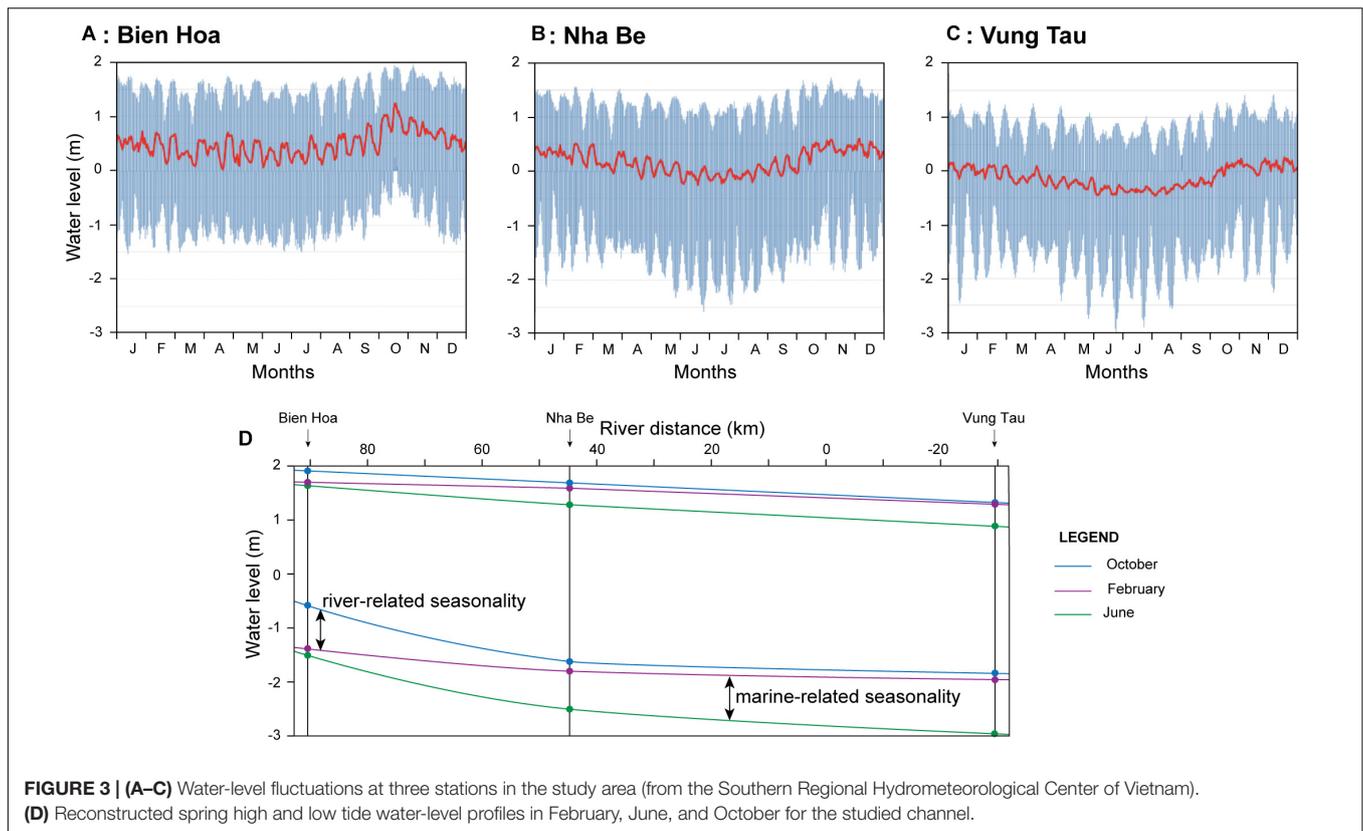
(**Figures 4G,H**, **5B,C**). An additional deeper area (confluence scour) and a sudden deepening of the channel are observed at the confluences of the Saigon River and the Vàm Có River, respectively.

DISCUSSION

River-Tidal and Valley Controls

Along the FMTZ of the DNRS, channel width, sinuosity, and bed elevation show mutual relationships and complex upstream to downstream trends linked to several factors, including the river-tidal dynamics and valley confinements, together with more local effects due to bifurcations and confluences (**Figure 4** and **Supplementary Table S1**). The part of the channel from which bathymetric data are available is constantly below the mean sea level and therefore falls within the backwater zone; however, it is not clear where the backwater limit is located and no clear evidence of a backwater control on the channel morphology is identified. The channel width is inversely proportionate to the channel sinuosity and channel bed elevation, whereas channel sinuosity and channel bed elevation are directly proportionate (**Figures 7A–C**). The studied channel shows a constant-width to seaward-widening trend typical of the FMTZ. The onset of widening is identified ∼100 km upstream of the river mouth, together with an abrupt decrease in sinuosity, whereas a seaward-shallowing trend is evident at least for the final 35 km of the channel. The seaward-widening and seaward-shallowing trends

in the downstream tract and the abrupt decrease in channel sinuosity are mainly due to the tidal dynamics; here, tidal water volume and current energy increase in a seaward direction causing the channel to become wider and straighter toward its mouth, whereas the tidal sediment import due to the tidal asymmetry makes the channel shallower (cf. Gugliotta and Saito, 2019; and references therein). In the downstream tract, the river dynamics still play a crucial role in contrasting and interacting with the tidal dynamics, making this tract of the FMTZ fundamentally different from purely tidal systems. Instead, the relatively constant channel width and sinuosity in the tract upstream of ∼100 km suggest a control due to the river dynamics; although tidal water-level fluctuations are still present herein, no clear evidence of a control of the tidal dynamics on the channel morphology is observed. Nonetheless, both the relationships between the three morphological parameters and their upstream to downstream trends show additional complications that are linked, in large part, to areas of valley widening or exit and presence of bedrock (**Figures 5A–C**, **7**). The part of the channel upstream of 75 km showing constant bed elevation is likely strongly controlled by the presence of bedrock at the channel bottom. The valley confinement and its variations in width play an important role in controlling the channel morphology along a large part of the studied channel. Valley-widening or -exit areas are characterized by an increase in channel width, high channel sinuosity, and variable channel bed elevation (**Figure 4**). Valley width shows a directly proportionate relationship with the three morphological parameters of the channel (**Figures 7D–F**).

FIGURE 4 | Measured and averaged valley width **(A,B)**, channel width **(C,D)**, channel sinuosity index **(E,F)**, and channel-bed elevation **(G,H)** along the Đồng Nai–Soài Rạp River.
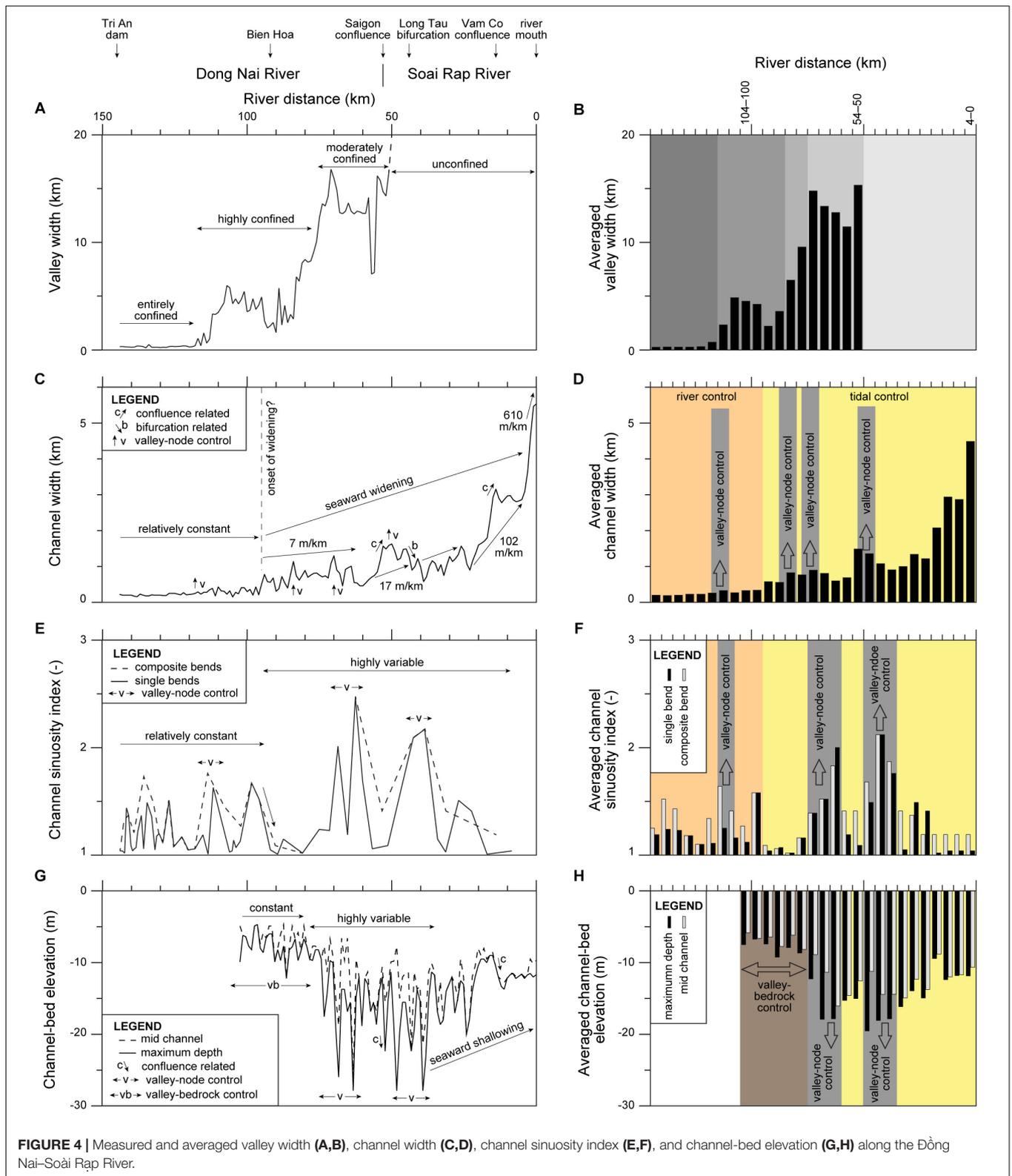
Many large river deltas, such as the Mekong and the Yangtze, have prograded for over 200 km during the last 8 kyr (Saito et al., 2001; Tamura et al., 2009) forcing the systems to exit their valleys

for a sufficient distance to clearly separate the valley-related signal from the river-tidal signal. Also, the large size of these systems and their high sediment discharge likely contributed to minimize
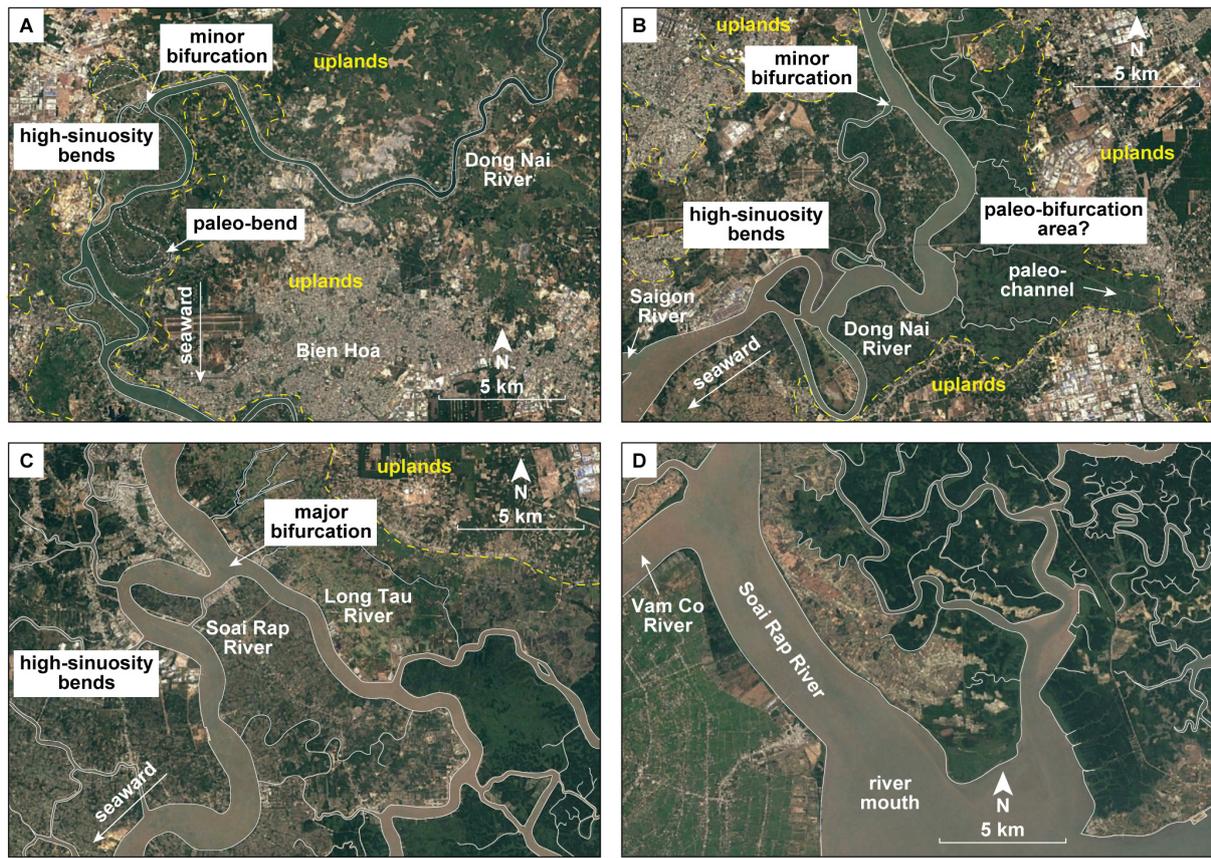
FIGURE 5 | Satellite images of selected parts of the Đồng Nai–Soài Rạp River (from Google Earth Pro, Landsat/Copernicus, 2016). (A–C) Areas of valley widening or exit and associated high-sinuosity bends and bifurcations. (D) River-mouth area. See **Figure 1C** for locations.
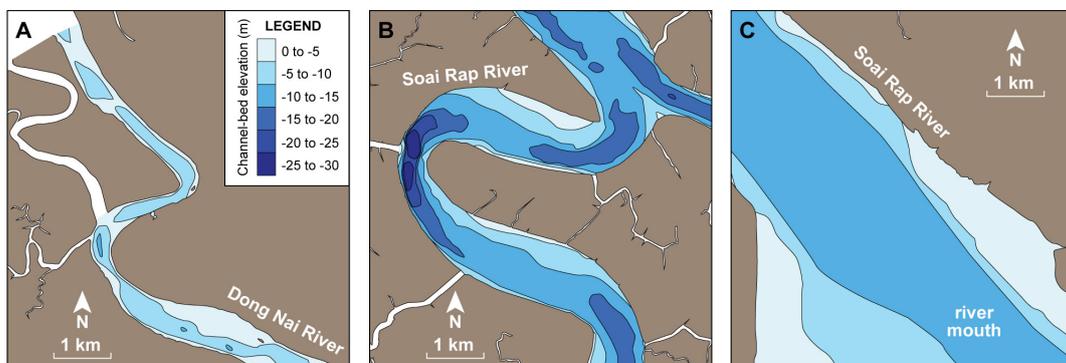
FIGURE 6 | Bathymetric maps of selected parts of the Đồng Nai–Soài Rạp River (modified from United States Army maps, Corps of Engineers, 1965). (A) Upstream part. (B) Intermediate part. (C) River-mouth area. See **Figure 1C** for locations.

local effects due to bifurcations, confluences, and valley or bedrock confinements, although these are still present (Gugliotta and Saito, 2019). On the other hand, small- to medium-scale river deltas like the DNRS have only partially exited their valleys, implying that the valley-related and river-tidal signals are mixed and of more difficult identification. The decoding of these more complex trends in small- to medium-scale systems is crucial in

order to fully understand the dynamics of river deltas and similar coastal environments.

The Importance of Valley-Related Nodes

The DNRS shows three areas of valley widening or exit that are characterized by high channel sinuosity, the presence of minor and major bifurcations that are not present in other parts

FIGURE 7 | (A–F) Plots showing the relationships between valley width, channel width, channel sinuosity, and channel bed elevation.

FIGURE 8 | Simplified model of the DNRS in plan view **(A)** and cross-section view **(B)** highlighting the river-tidal and valley-related controls.
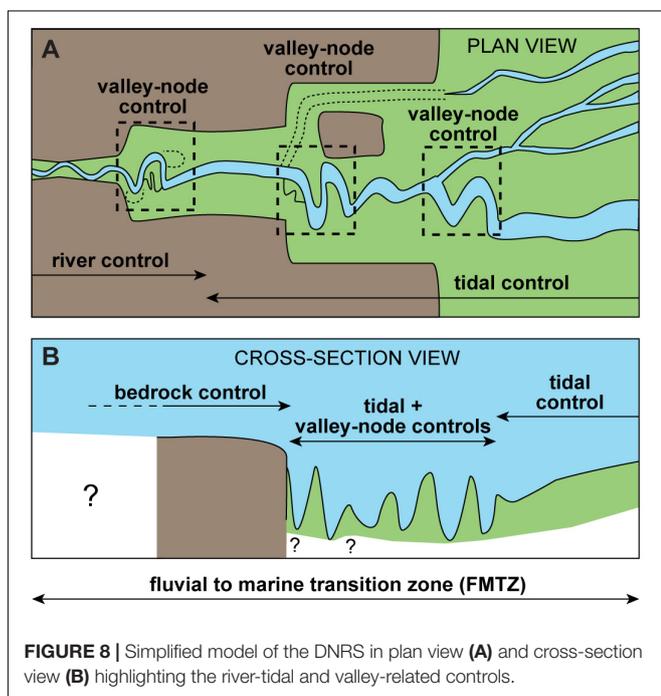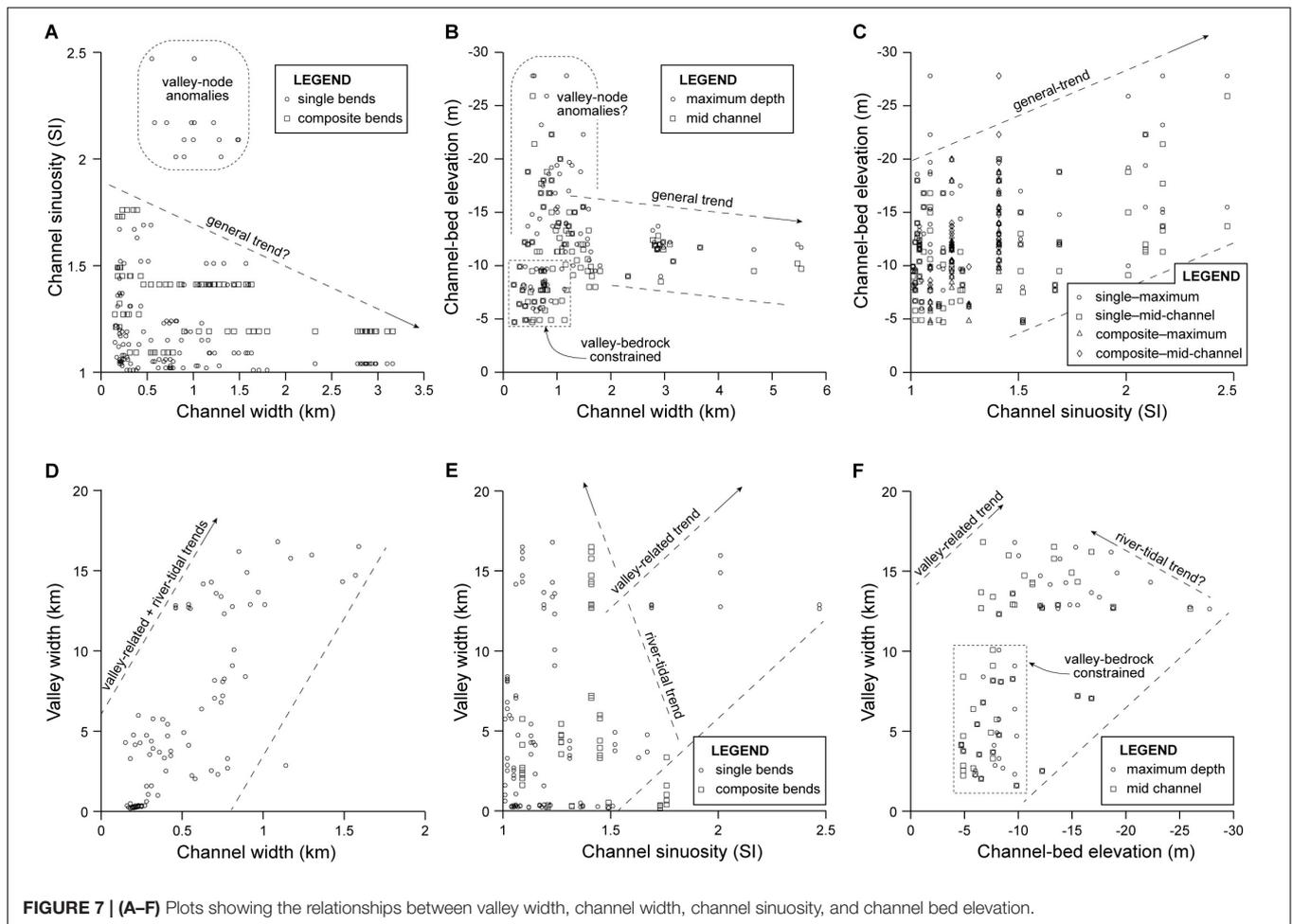
of the channel, and additional changes in channel width and bed elevation. These areas are considered here as important nodes in this system (**Figure 8**). The upstream node is located at approximately 120 km from the river mouth and it shows high-sinuosity bends and a minor bifurcation, in addition to two abandoned high-sinuosity paleo-bends (**Figure 5A**). The intermediate node is located at approximately 75 km, it is also characterized by the end of the bedrock control at the channel bottom (**Figures 4G,H**), and it shows high-sinuosity bends and a minor bifurcation, in addition to a major paleo-bifurcation (**Figure 5B**). The downstream node is located at approximately 50 km and it shows high-sinuosity bends and an active major bifurcation (**Figure 5C**). It should also be noted that these three nodes show different active and inactive features. The upstream and intermediate nodes show mostly abandoned bends and bifurcations and some active features, whereas the downstream node shows only active features. We suggest that the degree of activity and importance of these nodes likely varied through time, migrating from upstream to downstream due to the deltaic progradation. This implies that the downstream node is the most active and important one nowadays, whereas the other two might be considered as either subordinate or relict nodes. This inference is in line with the evolution of this

system reconstructed by Fujimoto et al. (2011) and with a similar seaward migration of nodes reported from the Huang He River delta (Ganti et al., 2014).

The definition of these valley-related nodes adds on existing literature highlighting the importance of similar areas in river deltas. This study is partially in line with Hartley et al. (2017), which reported that in numerous large river deltas the valley-exit areas are important nodes linked to major avulsions, increased channel migration, and changes in sediment dynamics. Our findings suggest that the valley-related nodes of the DNRS play an important role in controlling changes in channel morphology, possibly increasing migration and causing bifurcations, but do not necessarily imply significant amount of avulsion (defined as the process by which flow is diverted out of an established river channel into a new course on the adjacent floodplain; from Slingerland and Smith, 2004). Centennial- to millennial-scale river avulsions with formation of multiple lobes have been well documented in several river deltas, such as the Mississippi (Coleman et al., 1998), the Huang He (Saito et al., 2001), the Po (Correggiari et al., 2005), and the Danube (Giosan et al., 2005). This concept is often applied to other river deltas or models, however, many tide-dominated and/or wave-dominated deltas, such as the Yangtze (Hori et al., 2002), the São Francisco (Dominguez, 1996), and the Mekong (Tamura et al., 2012), do not show significant avulsion during their Holocene history. In the DNRS, bifurcations are rare and might have formed for reasons different from avulsion, such as the growth of bars that caused the subdivision of the channel. Avulsions seem to be either absent or occasional compared to the avulsing systems mentioned above; thus, we suggest that these valley-related nodes should not be considered as avulsion nodes.

CONCLUSION

Along the FMTZ of the DNRS, channel width, sinuosity, and bed elevation show mutual relationships and complex upstream to downstream trends linked to several factors, including river-tidal dynamics and valley confinements, together with more local effects due to bifurcations and confluences. Tidal dynamics are mainly responsible for the seaward-widening and seaward-shallowing trends and the abrupt decrease in channel sinuosity

observed in the downstream tract of the channel, whereas the relatively constant channel width and sinuosity in the upstream tract suggest a control of the river dynamics. The valley confinement and the bedrock at the channel bottom play an important role in controlling the channel morphology along a large part of the studied channel. Valley-widening or valley-exit nodes are characterized by an increase in channel width, high channel sinuosity, variable channel bed elevation, and bifurcations. Valley-related nodes also show different active and inactive features, implying that the degree of activity and importance of these nodes likely varied through time, migrating from upstream to downstream due to the deltaic progradation.

DATA AVAILABILITY

All datasets for this study are included in the manuscript and/or the **Supplementary Material**.

AUTHOR CONTRIBUTIONS

MG primarily designed the study, collected the data, wrote the manuscript, and prepared the figures. YS contributed to the writing, organizing the manuscript, and discussion. TKOT and VLN provided some of the data and contributed to the writing and discussion.

FUNDING

SUPPLEMENTARY MATERIAL

The Supplementary Material for this article can be found online at: https://www.frontiersin.org/articles/10.3389/feart.2019.00202/full#supplementary-material

REFERENCES

Coleman, J. M., Roberts, H. H., and Stone, G. W. (1998). Mississippi river delta: an overview. *J. Coast. Res.* 14, 699–716.

Correggiari, A., Cattaneo, A., and Trincardi, F. (2005). The modern Po Delta system: lobe switching and asymmetric prodelta growth. *Mar. Geol.* 222, 49–74. doi: 10.1016/j.margeo.2005.06.039

Dalrymple, R. W., and Choi, K. (2007). Morphologic and facies trends through the fluvial-marine transition in tide-dominated depositional systems: a schematic framework for environmental and sequence-stratigraphic interpretation. *Earth Sci. Rev.* 81, 135–174. doi: 10.1016/j.earscirev.2006.10.002

Dao, T. S., Cronberg, G., Nimptsch, J., Do-Hong, L. C., and Wiegand, C. (2010). Toxic cyanobacteria from Tri an reservoir, Vietnam. *Nova Hedwigia* 90, 433–448.

Dominguez, J. M. L. (1996). The Sao Francisco strandplain: a paradigm for wave-dominated deltas?," in *Geology of Siliciclastic Shelf Seas*, Vol. 117, eds M. De Batist and P. Jacobs (London: Geological Society London Special Publications), 217–231. doi: 10.1144/gsl.sp.1996.117.01.13

Fujimoto, K., Umitsu, M., Nguyen, V. L., Ta, T. K. O., Kawase, K., Huynh, D. H., et al. (2011). "Geomorphological evolution and mangrove habitat dynamics related to Holocene sea-level changes in the Northern Mekong River Delta and the Dong Nai River Delta, Southern Vietnam," in *River deltas: Types, Structures and Ecology*, ed. P. E. Schmidt (Hauppauge, NY: Nova Science Publishers, Inc.), 125–141.

Ganti, V., Chu, Z., Lamb, M. P., Nittrouer, J. A., and Parker, G. (2014). Testing morphodynamic controls on the location and frequency of river avulsions on fans versus deltas: Huanghe (Yellow River). *China Geophys. Res. Lett.* 41, 7882–7890. doi: 10.1002/2014gl061918

Giosan, L., Donnelly, J. P., Vespremeanu, E., Bhattacharya, J. P., Olariu, C., and Buonaiuto, F. S. (2005). "River delta morphodynamics: examples from the Danube delta," in *River Deltas–Concepts, Models, and Examples*, eds L. Giosan and J. P. Bhattacharya (Tulsa, OK: SEPM Society for Sedimentary Geology), 393–411. doi: 10.2110/pec.05.83.0393

Gugliotta, M., and Saito, Y. (2019). Matching trends in channel width, sinuosity, and depth along the fluvial to marine transition zone of tide-dominated river deltas: the need for a revision of depositional and hydraulic models. *Earth Sci. Rev.* 191, 93–113. doi: 10.1016/j.earscirev.2019.02.002

Gugliotta, M., Saito, Y., Nguyen, V. L., Ta, T. K. O., Nakashima, R., Tamura, T., et al. (2017). "Process regime, salinity, morphological, and sedimentary trends along the fluvial to marine transition zone of the mixed-energy Mekong river Delta, Vietnam," in *Sediment- and Hydro-Dynamics of the Mekong Delta: From Tidal River to Continental Shelf*, Vol. 147, eds A. S. Ogston, M. A. Allison, J. C. Mullarney, and C. A. Nittrouer (Amsterdam: Elsevier), 7–26. doi: 10.1016/j.csr.2017.03.001

Guo, L., van der Wegen, M., Roelvink, J. A., and He, Q. (2014). The role of river flow and tidal asymmetry on 1-D estuarine morphodynamics. *J. Geophys. Res.* 119, 2315–2334. doi: 10.1002/2014jf003110

Hartley, A. J., Weissmann, G. S., and Scuderi, L. (2017). Controls on the apex location of large deltas. *J. Geol. Soc.* 174, 10–13. doi: 10.1144/jgs2015-154

Hennig, J., Breitfeld, H. T., Gough, A., Hall, R., Long, T. V., Kim, V. M., et al. (2018). U-PB zircon ages and provenance of upper cenozoic sediments from the Da Lat zone, SE Vietnam: implications for an intra-Miocene unconformity and paleo-drainage of the proto–Mekong River. *J. Sediment. Res.* 88, 495–515. doi: 10.2110/jsr.2018.26

Hori, K., Saito, Y., Zhao, Q., and Wang, P. (2002). Architecture and evolution of the tide-dominated Changjiang (Yangtze) river delta, China. *Sediment. Geol.* 146, 249–264. doi: 10.1016/s0037-0738(01)00122-1

Kästner, K., Hoitink, A. J. F., Vermeulen, B., Geertsema, T. J., and Ningsih, N. S. (2017). Distributary channels in the fluvial to tidal transition zone. *J. Geophys. Res.* 122, 696–710. doi: 10.1002/2016jf004075

Kitazawa, T., Nakagawa, T., Hashimoto, T., and Tateishi, M. (2006). Stratigraphy and optically stimulated luminescence (OSL) dating of a Quaternary sequence along the Dong Nai River, southern Vietnam. *J. Asian Earth Sci.* 27, 788–804. doi: 10.1016/j.jseaes.2005.08.001

La Croix, A. D., Dashtgard, S. E., Gingras, M. K., Hauck, T. E., and MacEachern, J. A. (2015). Bioturbation trends across the freshwater to brackish-water transition in rivers. *Palaeogeogr. Palaeoclimatol. Palaeoecol.* 440, 66–77. doi: 10.1016/j.palaeo.2015.08.030

Nguyen, T. T., Némery, J., Gratiot, N., Strady, E., Tran, V. Q., Nguyen, A. T., et al. (2019). Nutrient dynamics and eutrophication assessment in the tropical river system of Saigon–Dongnai (southern Vietnam). *Sci. Total Environ.* 653, 370–383. doi: 10.1016/j.scitotenv.2018.10.319

Nienhuis, J. H., Hoitink, A. J. F., and Törnqvist, T. E. (2018). Future change to tide-influenced deltas. *Geophys. Res. Lett.* 45, 3499–3507. doi: 10.1029/2018gl077638

Saito, Y., Yang, Z., and Hori, K. (2001). The Huanghe (Yellow River) and Changjiang (Yangtze River) deltas: a review on their characteristics, evolution and sediment discharge during the Holocene. *Geomorphology* 41, 219–231. doi: 10.1016/s0169-555x(01)00118-0

Sassi, M. G., Hoitink, A. J. F., Brye, D. B., and Deleersnijder, E. (2012). Downstream hydraulic geometry of a tidally influenced river delta. *J. Geophys. Res. Earth Surf.* 117:F04022.

Slingerland, R., and Smith, N. D. (2004). River avulsions and their deposits. *Ann. Rev. Earth Planetary Sci.* 32, 257–285. doi: 10.1146/annurev.earth.32.101802.120201

Tamura, T., Saito, Y., Nguyen, V. L., Ta, T. K. O., Bateman, M. D., Matsumoto, D., et al. (2012). Origin and evolution of interdistributary delta plains; insights from Mekong river delta. *Geology* 40, 303–306. doi: 10.1130/g32717.1

Tamura, T., Saito, Y., Sieng, S., Ben, B., Kong, M., Sim, I., et al. (2009). Initiation of the Mekong River delta at 8 ka: evidence from the sedimentary succession in the Cambodian lowland. *Quat. Sci. Rev.* 28, 327–344. doi: 10.1016/j.quascirev.2008.10.010

Yang, H. F., Yang, S. L., and Xu, K. H. (2017). River-sea transitions of sediment dynamics: a case study of the tide-impacted Yangtze river estuary. *Estuar. Coast. Shelf Sci.* 196, 207–216. doi: 10.1016/j.ecss.2017.07.005